Published in Earth and Planetary Science Letters 240 : 764-773, 2005,
which should be used for any reference to this work

Electrical structure of the tectonically active Kalabsha Fault, Aswan, Egypt

Mahmoud Mekkawi [a], Pierre-André Schnegg [a,*], Tarek Arafa-Hamed [b], Essam Elathy [b]

[a] *Institut de Géologie, Université de Neuchâtel, Neuchâtel, Switzerland*
[b] *National Research Institute of Astronomy and Geophysics, Helwan, Egypt*

Received 31 January 2005; received in revised form 17 May 2005; accepted 22 September 2005
Available online 10 November 2005
Editor: V. Courtillot

Abstract

In this work, we use the magnetotelluric (MT) method to detect geoelectrical conductivity anomalies in the Earth's crust and link them to local seismic activity. This application affords the unusual opportunity to study the percolation of water from a lake into a fault system and its effect on the induced seismicity. MT measurements were carried out in the period range 0.0046–420 s at nine sites along a 15 km-long North–South profile crossing the Kalabsha Fault, on the western bank of Lake Aswan. Data were analysed by 2D simultaneous inversion of both polarisations. The resulting model is compared with the local seismicity map and reveals the conductive signature of the fault, as well as geological and tectonic stresses prevailing in the Aswan area. Our MT investigations show the following features:

The measured MT strike aligns with the seismic epicentre axis corresponding to the Kalabsha Fault.

While crossing the Fault, enhanced conductivity is found down to depths of 5 km on a 1–2 km profile segment.

At mid-crustal depths (20 km), a very high conductive body is found to coincide with the main seismic cluster in the Aswan area.

These observations indicate that seismic activity and high electrical conductivity are related. The link between them is the presence of crustal fluids which are presumably the cause of the high conductivity observed. Their presence is also required to trigger the observed seismicity. In addition, we explain the lower conductivity of the local upper crust in terms of stress-modulated rock porosity. We believe that these results are of general significance, as they could explain the mid-crustal seismicity of tectonically active zones.

Keywords: magnetotelluric surveys; active fault; reservoir-induced seismicity; Egypt

1. Introduction

MT measurements were carried out in the area of Wadi Kalabsha about twenty years after the occurrence of the November 14, 1981 earthquake. This earthquake was measured 5.4 on the Richter scale, with its epicentre occurring about 60 km to the south of the High Aswan Dam. This rock-fill dam across the Nile River (111 m high, crest length: 3830 m), was completed in 1970 and impounds a reservoir with a gross capacity of 169 billion cubic metres, Lake Nasser (or Lake Aswan). Seasonal water level fluctuations reach 5 m. Lake Aswan provides Egypt with hydroelectric power,

* Corresponding author. Tel.: +41 32 718 26 76; fax: +41 32 718 26 01.
E-mail address: pierre.schnegg@unine.ch (P.-A. Schnegg).

water supply and protects the country from high magnitude flood events. Lake Aswan now extends over 350 km upstream along the Nile River in Egypt and 150 km in Sudan. Consequently, an earthquake event damaging the dam could pose a severe threat to the economic and social well being of the downstream population. Tectonic activity is thought to result from the impoundment of the lake [1,2].

Many areas in tectonically active regions have previously been investigated with MT. In Africa, rift valleys have received particular attention [3–8]. Anomalous crustal conductors are sometimes related to seismic activity. The pioneering MT work recently completed on the San Andreas Fault provided the impulse for the current research [9–13]. A recent revaluation of this work has been published [14]. In the Himalaya of Central Nepal, microseismicity and metamorphic fluids were invoked to explain the anomalously high conductivity in the middle crust [15]. Similar conclusions were drawn in an MT study around the Gulf of Corinth [16]. In India, geophysical investigations in the vicinity of the deadly Latur earthquake [17] provided a precursory approach to our own research and supported the presence of fluids as the reason for anomalous conductivity that triggered the release of seismic energy.

Annual level variations in Lake Aswan have been well correlated with the local seismic activity [18], suggesting that a transfer of hydrostatic pressure occurs through the faulted rocks. The goal of the current research is to confirm the presence of crustal fluids and thus, to explain the triggering mechanism for earthquakes occurring in this seismically active area; this was achieved by looking for a typical conductive signature of transcurrent faults such as the Kalabsha Fault [19].

2. Geological and tectonic settings

In Egypt the Arabo-Nubian massif is bisected by the Red Sea rift and its continuation (as continental rifts) into the Gulfs of Suez and Aqaba. The basement occupies 10% of Egypt surface (Fig. 1a). Recent tectonic structures represent the most active regions of the Precambrian shield outcrop to their greatest extent in Ethiopia, Sudan, the eastern part of Egypt and Sinai [20].

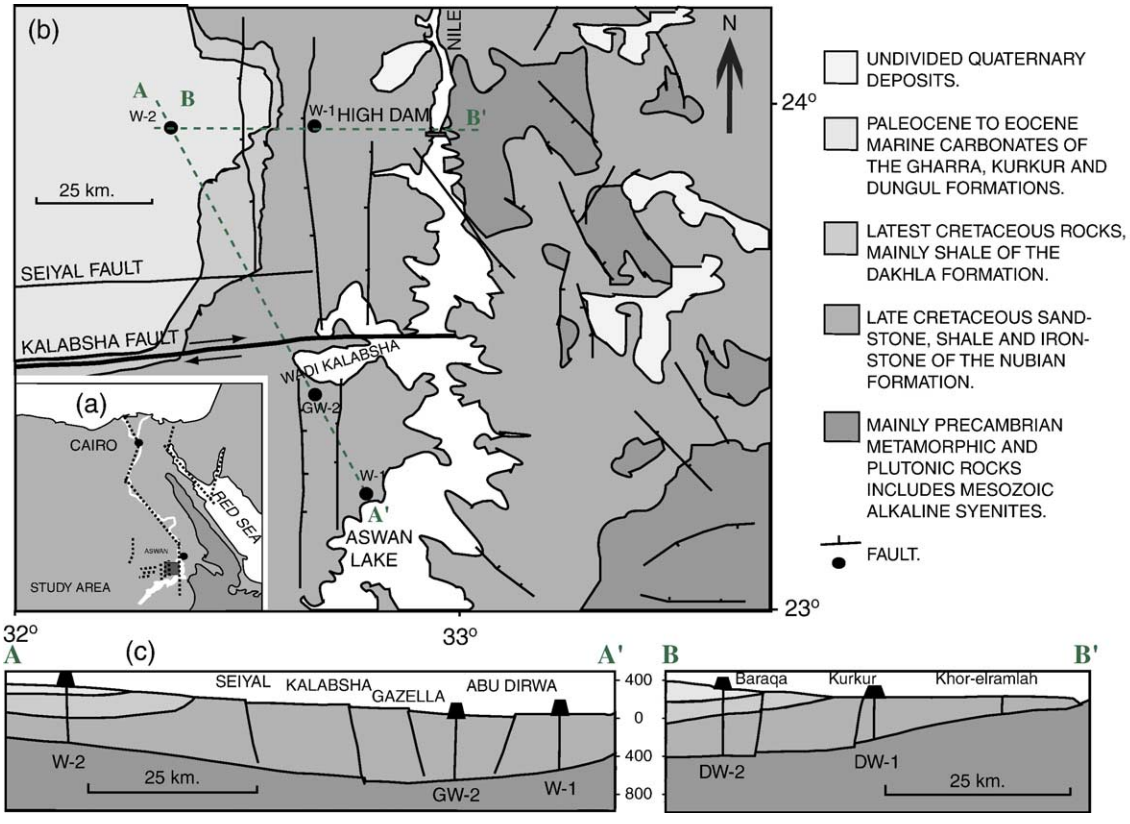

Fig. 1. (a) Location map of the study area with main regional faults and basement distribution [20]. (b) Regional geological and tectonic settings of Aswan area. (c) Borehole location [21].

The Precambrian basement is unconformably overlaid by the Nubian formation whose sediments range in age from Late Cretaceous to Eocene (Fig. 1b). Kurkur and Gurra formations locally overlie the Nubian formation in some places. Finally, Quaternary deposits consist of limestone and Nile alluvial deposits [21,22]. Geomorphologically, the area around Aswan is almost flat, with relief varying from 150 to 350 m above sea level. Topography is complicated by faults and the presence of several alkali granites and a syenite ring complex.

Tectonic features, dominated by EW and NS fault systems, as well as a regional uplift, characterize the northern part of Lake Aswan [23]. Geological data of these features indicate that right-lateral strike-slip movement is the dominant mechanism along the Kalabsha Fault zone [29]. Igneous intrusions and associated contact metamorphism may be found in a few localities on the western side of Lake Aswan. These units constitute the main geological formations encountered on the eastern side of the lake. Information from the boreholes indicates that the average thickness of the Nubian formation and whole sedimentary column is approximately 500 m (Fig. 1c).

A telemetry network (Aswan Seismograph Network, ASN) was established around the northern part of Lake Aswan in July 1982. Each field station is equipped with a single-component vertical seismometer model S13, radio-telemetry and solar panels. Since 1989, the ASN consists of 13 field stations. As mentioned in the Introduction, Mekkawi et al. [18] analyzed the Aswan seismicity patterns observed during the period 1982–2001 in an attempt to explain how water level loading could drive the seismicity. The Aswan seismicity may be subdivided into shallow (0.1–15 km) and deep (>15 km) seismic zones (Fig. 2). These two zones behave differently over time, as mapped by seismicity rate, depth migration, b-value, and spatial clustering. Analyses of these data suggest that the Aswan seismicity patterns emerge from the interplay between induced earthquakes themselves and the water level fluctuations. Since the Kalabsha Fault runs across the bottom of the lake, we suspected that some water was percolating into the fault. Strong evidence of this was found in the correlation between water level (the cause) and seismicity rate (the effect). Delays of 60 and 120 days between the cause and its effect were observed for shallow and deep earthquakes, respectively. Consequently our MT profile was carried out across the Kalabsha Fault in order to confirm the presence of water and to assess the role of crustal fluids in triggering the observed seismicity.

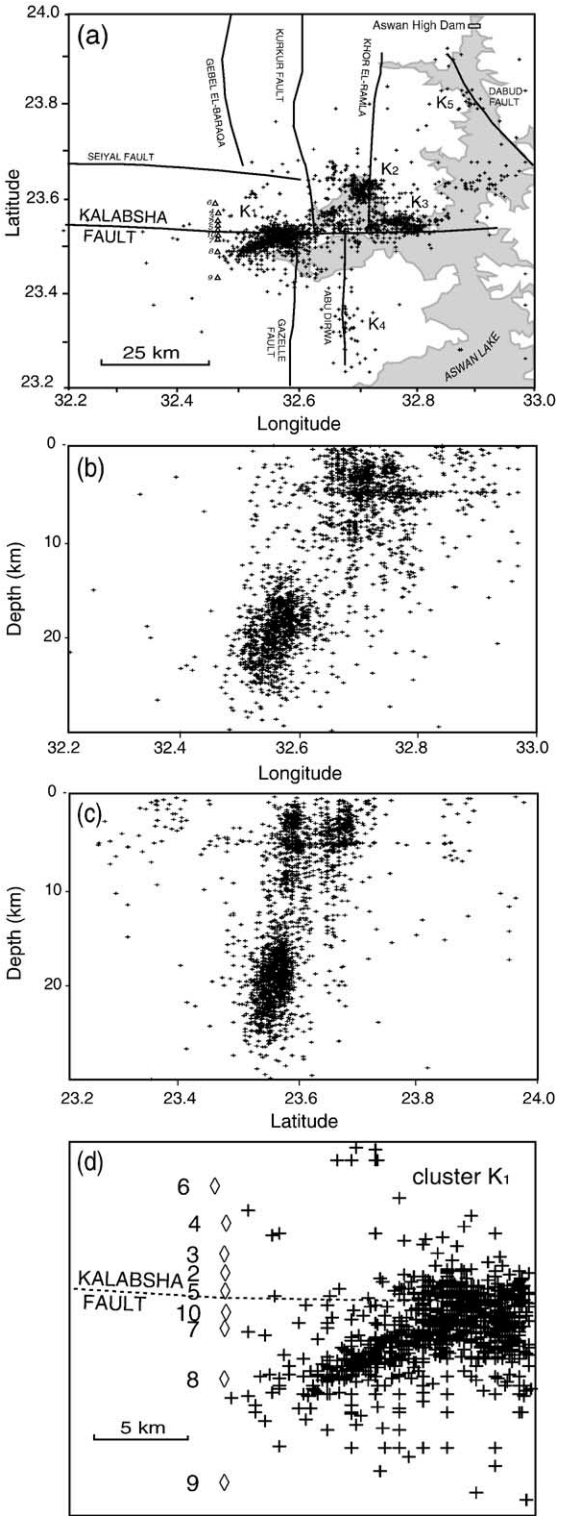

Fig. 2. (a) Location map of Kalabsha Fault and spatial distribution of earthquakes in Aswan area [18]. The K_i denote cluster zones. MT profile is shown crossing the fault. (b, c) Epicentres and focal depths for $M>=2$. (d) Detailed MT profile view.

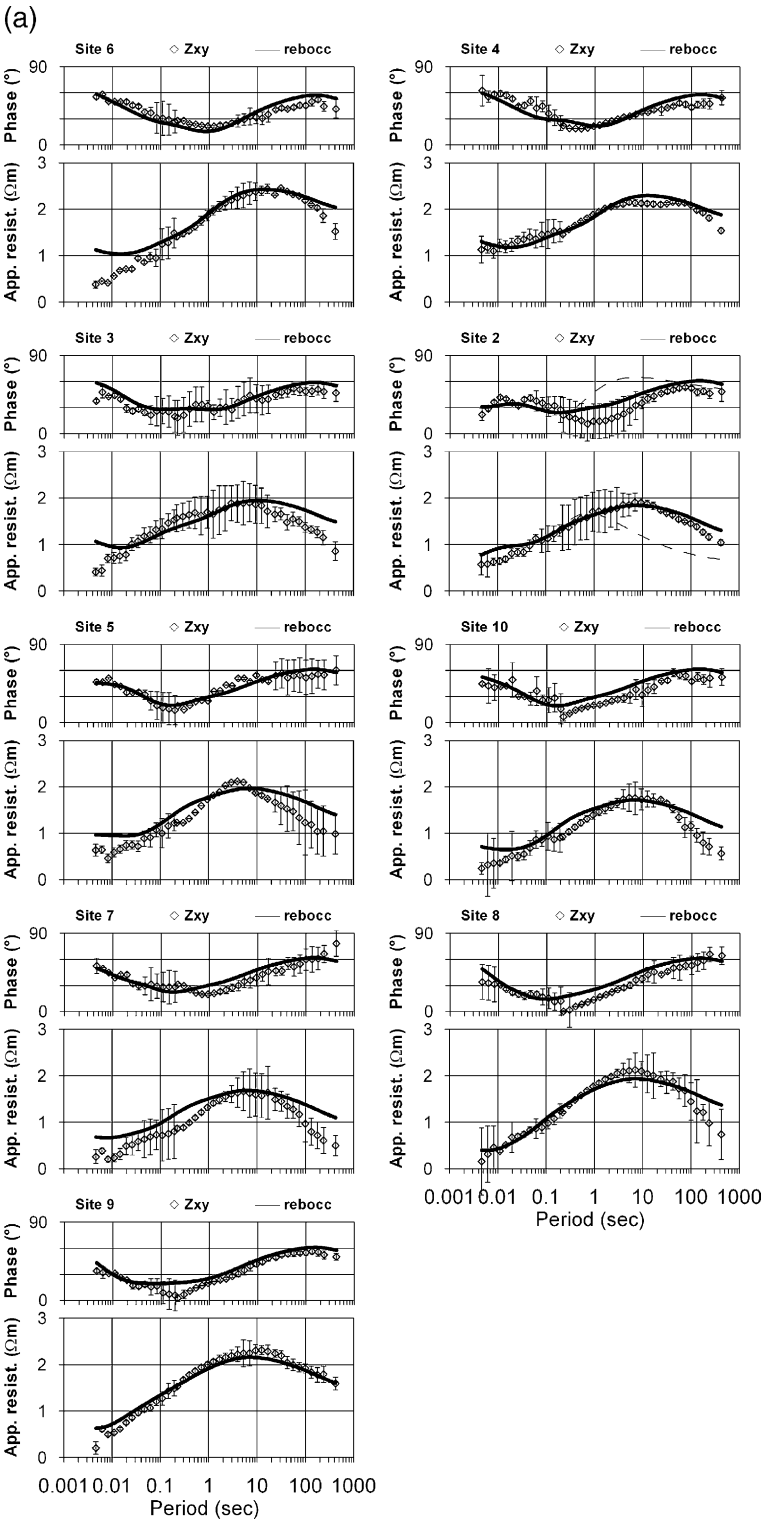

Fig. 3. (a) Observed apparent resistivity and phase with response of 2D model for TM mode. On site 2, model response with resistivity of the deep part of the model (>8 km) fixed to a constant value of 20 Ωm (broken line). (b) Observed apparent resistivity and phase with response of 2D model for TE mode. On site 2, model response with resistivity of the deep part of the model (>8 km) fixed to a constant value of 20 Ωm (broken line).

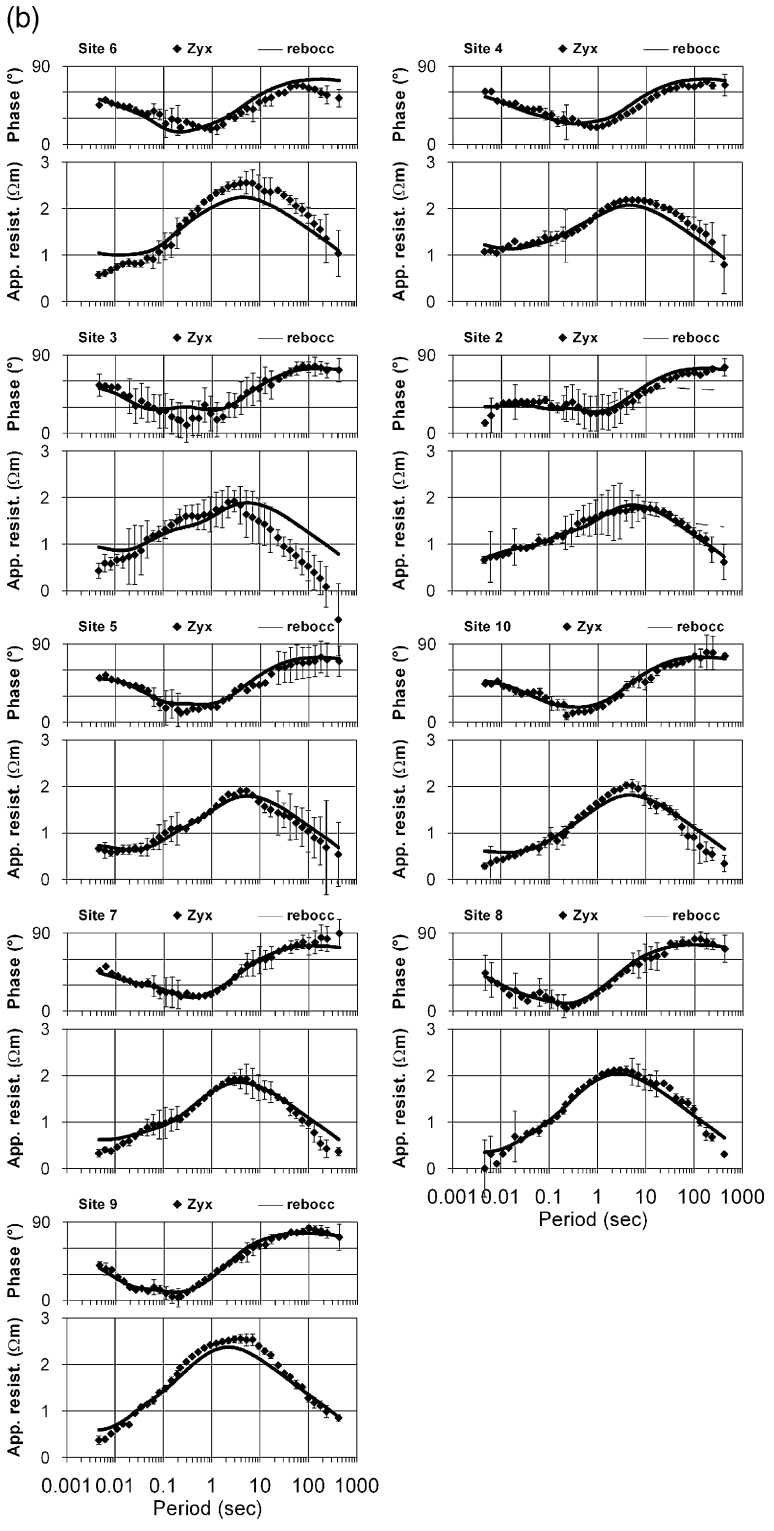

Fig. 3 (*continued*).

3. Practical aspects of data acquisition and MT response function estimation

MT data acquisition in the Kalabsha area took place over two weeks in September/October 2001. Field work was carried out during the low water season in Wadi Kalabsha in order to increase the profile coverage in an otherwise flooded area. MT measurements were carried out in the period range 0.0046–420 s at nine sites in a North–South profile crossing the Kalabsha Fault (Fig. 2). The length of the profile was 15 km. Unfortunately it was not possible to set up the profile axis more to the east, across the main earthquake cluster K_1, since the cluster is now permanently covered by the lake. Two MT stations constructed by the University of Neuchâtel recorded continuous data during two days. Every day, one station was dismantled and re-installed at a neighbouring site. Two different sets of magnetic induction coils [24] were employed. Magnetic field variations of short periods (audio magnetotellurics, AMT) were measured with ECA CM16 coils, whereas longer periods (MT) used ECA CM11E coils. These instruments made it possible to switch between the overlapping AMT and MT modes. The telluric electrodes consisted in acrylic tubes ended with porous material. Inside the tube a non-polarisable Ag–AgCl electrode designed for ocean studies [25] was immersed in a saturated KCl solution. The soil was extensively watered. No contact problem occurred owing to the high input impedance of the telluric preamplifiers. The telluric lines were oriented in the direction of magnetic north and in the corresponding perpendicular (East–West) direction. Magnetic declination was less than 3°. The length of the telluric lines was either 50 or 100 m, depending on the topography. Unfortunately, heat and dust prevented measurement of the vertical magnetic component, since the H_z coil had to be used as a replacement for the faulty horizontal one. MT response function estimation was carried out with the single station, least-squares scheme using data dispersion as a selection criterion [26]. Fig. 3a–b show the observed apparent resistivity and phase of TM and TE modes. Unfortunately, the first four days of field work were characterised by a low magnetospheric activity. For this reason, in an otherwise man-made noise-free area, the three first sites display large error bars at periods around 1 s (actually, site 1 was even discarded).

4. MT transfer function of Kalabsha area

Before modelling the resistivity structures, we studied impedance tensors for dimensionality and strike direction of the geoelectrical structure. At all sites over longer periods ($T>1$ s) skew was found to be below 0.2 except for site 3 (Table 1). Consequently the data were treated as 2D and handling in 3D was not required. The question arises of a possible 3D effect of the nearby Lake Nasser. However, considering the low average water conductivity (250 μScm^{-1}, corresponding to a resistivity of 40 Ωm), there is virtually no electrical contrast with the subsurface value (<30 Ωm) and therefore, there cannot be any significant effect.

Table 1
Example of skew vs. period T at three sites

T (s)	Site 9	Site 3	Site 6
0.2	0.02	0.72	0.03
0.4	0.01	0.88	0.12
0.7	0.02	1.00	0.10
1.2	0.01	0.83	0.11
2.2	0.04	0.53	0.15
3.9	0.06	0.54	0.07
7.0	0.05	0.67	0.12
12.5	0.05	0.38	0.06
22.2	0.08	0.24	0.14
52.6	0.14	0.27	0.15

To determine the geoelectrical strike Groom-Bailey (GB) decomposition scheme [27] was applied to the profile. As could be expected for a tabular subsurface, variability of the strike angle is large at short periods (<1 s) even when the twist and shear angles are relatively stable with frequency. For the long period range the GB decomposition yields twist and shear angles close to zero, and a regional strike of N60°E, i.e., 15° off the geological strike of the Kalabsha Fault as observed at ground surface. However, closer inspection of the earthquake distribution presented in Fig. 2a indicated that the epicentres do not align strictly with the surficial track of the fault. This is a feature of *en échelon* faults. Interestingly, the epicentre axis is oriented along the geoelectrical strike. After rotating the impedance tensors of all periods and all sites into the new coordinate axis, 2D inversion was carried out, with TE mode identified as the Z_{yx} element of the impedance.

5. Two-dimensional magnetotelluric modelling of the Kalabsha conductivity anomaly

The inversion program REBOCC, an inversion scheme for 2D magnetotelluric data to invert TE and TM apparent resistivity and phase simultaneously was employed [28]. Field data consists of TE and TM mode responses at 40 periods extending from 0.0046 to 420 s.

The REBOCC initial model was chosen as a 10 Ωm half-space with 34 layers (plus 10 air layers for TE mode). The data did not show noticeable static shift. After 21 iterations the inversion result yielded an RMS misfit value of 3.5. Observed apparent resistivity and phase of TM and TE modes are shown in Fig. 3a–b, along with final model response (Fig. 4).

The fit of the model response to the observed data is generally satisfactory for both polarisations. Simultaneous modelling of TE and TM modes certainly provides better model constrains than single mode, so long as the data in both modes are of equivalent quality. However, to check the model sensitivity, two tests were carried out. In the first, single-mode data were modelled. RMS misfits for TM and TE modes were found at 3.2 and 4.5. The main features of the combined-mode model were present: Conductive subsurface, resistive upper-crust, and conductive 2D body between sites 4 and 5, extending from the surface down to the middle crust. Two noticeable differences were observed: In TE

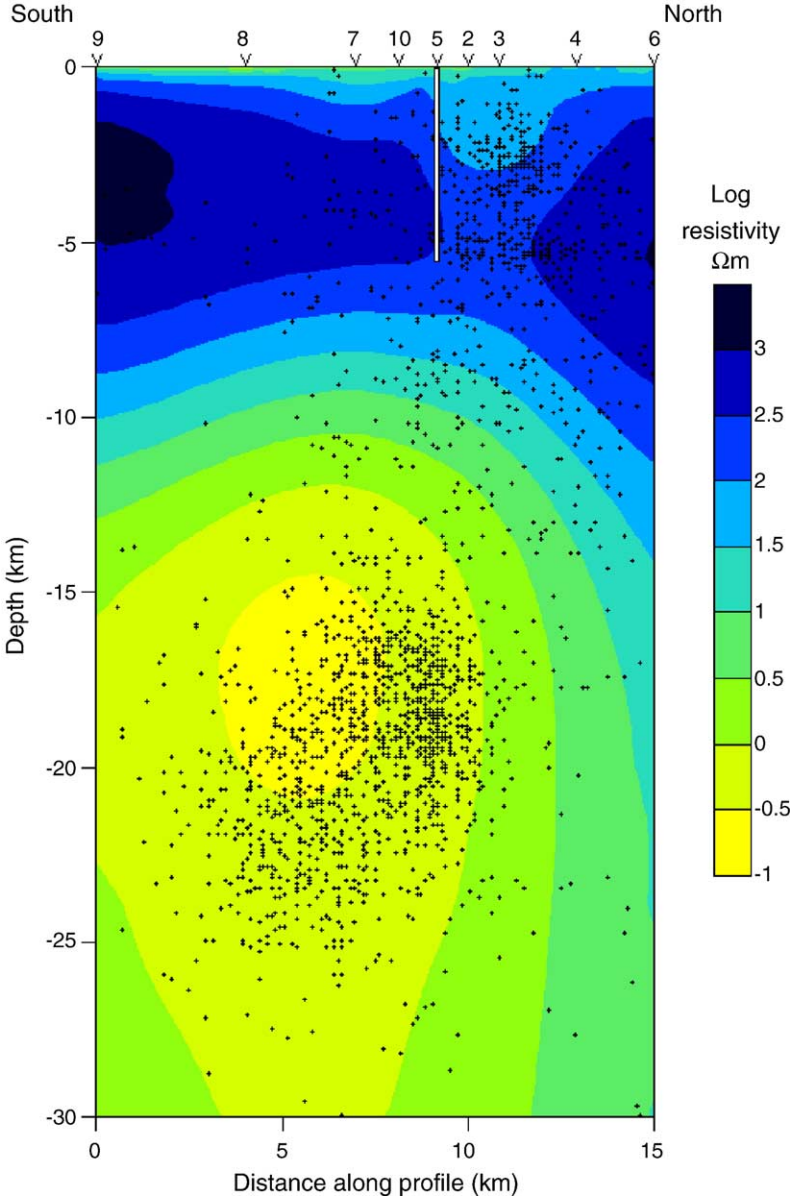

Fig. 4. Final 2D model based on MT data of both polarizations TE and TM along a profile crossing the Kalabsha fault (white vertical line) in North–South direction. The symbols above the model identify the MT sites. The location of the profile and the measurement sites are shown in Fig. 3. Earthquake hypocenters are shown as black dots.

mode, the barycentre of the mid-crust conductive body was located between sites 7 and 8 at a depth of 10 km and displayed a resistivity of 0.1 Ωm. In TM mode, this body was centred between sites 3 and 4 and extended to a depth of 25 km with a higher resistivity (2 Ωm). In either cases the 2D conductive body was required for a good data fit. This was confirmed in a second test, where the resistivity of the deep part of the model (>8 km) was fixed to a constant value of 20 Ωm. The model response is plotted for site 2 in Fig. 3a–b.

6. Discussion

A tentative image of the final Kalabsha geoelectrical 2D model correlated with the distribution of earthquake hypocentres is presented in Fig. 4. Because seismic clusters K_1 and K_3 seem to belong to the Kalabsha Fault (Fig. 2a), all earthquake foci from the catalogue of 1982–2001 events for these clusters were projected on the MT section of Fig. 4 in the direction of the fault plane, i.e., the N60°E direction. Selecting the dataset of the entire period and not only the more recent earthquakes was meaningful, since each earthquake could be considered a marker for the presence of crustal fluid.

Further away from the fault, the model shows an upper crust resistivity in excess of 1000 Ωm on either side. This large value is consistent with fissure-free basement rocks. The influence of stress could be related to the two lateral resistive zones (Fig. 4) in terms of stress-modulated porosity, as follows:

1) Vertical compressional stress due to loading of Lake Aswan increases pore fluid pressure.
2) The fault system of Wadi Kalabsha is strike-slip and occurs under the influence of maximum compressional stress in the NW–SE direction [29]. This stress may be the cause of the pore closure, with a reduction in the rock conductivity.

In contrast, the top layer is a good conductor and has a resistivity of less than 30 Ωm and about 500 m thickness, resulting from the high porosity in the Nubian sandstone and water percolation during the season when the lake covers the area. Evans et al. [30] estimated aquifer parameters through the application of time series analysis to water level data from boreholes. They mentioned that the stratigraphy of the Nubian formation in the area consisted of three horizontal units with a combined thickness of 400 m. The lowermost unit, overlying the granite basement is an aquifer made of fluvial sandstones and has an elevated horizontal permeability over an area of several kilometres. The intermediate unit is an aquiclude that extends unbroken under the lake and leaks water to the underlying sandstone at periods of several years. The uppermost unit is an unconfined aquifer, which consists of sandstone with interspersed clay lenses with a porosity of 25–30%. This sandstone has an elevated permeability over a large area.

The 2D MT response of the area can be attributed to a narrow (~3 km), deep-reaching low-resistivity (~30 Ωm) zone that extends vertically between sites 2 and 3 from the surface to a depth of 5 km below ground, close to the Kalabsha Fault. The conductor width is well constrained by adequate MT site distribution every 1–2 km. This could reflect the geoelectrical response of crustal fluids trapped in the fractured rocks in the fault zone.

Fracture porosity in the fault zone can be estimated from resistivities ρ_m obtained in the MT mode (Depth: 0, $\boldsymbol{\rho_m}$=6 Ωm, Depth: 3 km, $\boldsymbol{\rho_m}$=30 Ωm). In a rock with a porosity estimated by Evans et al. [30] at 28%, a resistivity of 6 Ωm is achieved with ρ_w=0.5 Ωm interstitial water. From this result we conclude that the ρ=30 Ωm fault zone must have a porosity of 12%. Similarly, the unfaulted basement has an elevated resistivity of 130 Ωm, corresponding to a much lower porosity (6%, and even less since dry sandstone may display resistivity close to 200 Ωm).

Shallow earthquakes (<15 km, Fig. 4) nicely correlate with the location of the vertical conductor. The fault area is known to be highly fractured [21]. Water penetrating to the fractured basement and along the fault plane could cause a pore pressure build-up and trigger seismic activity. The increase in pore pressure can drive a fault system to failure by the mechanism of dilatancy. Studies on some recent earthquakes in the San Andreas Fault area suggest that stress changes as low as 0.1 bar are sufficient to induce failure in critically stressed zones [31].

A very low resistivity (<1 Ωm) conductive feature extends across the basement down to the centre of seismic cluster K_1 (~15–20 km) into the middle crust. The fact is that the deepest parts of this body cannot be well constrained by inversion due to the low resistivity region overlying it. For instance, there is a 3 km offset between the barycentre of earthquakes and the conductive zone in the model. An attempt to interpret such non-vanishing offset as a horizontal cluster migration could be illusory when considering the significant differences between TM and TE models, particularly the horizontal location of this conductive zone (see discussion in Section 5). It should also be kept in mind that the MT profile had to be moved 4 km to the west of the

seismic cluster because of the presence of the Lake, resulting in a reduced positioning accuracy due to the parallax. Nonetheless the existence of fluids in the porous medium is required to simultaneously explain seismicity triggering and low resistivity. Mekkawi et al. [18] showed that during a period of ten years after the occurrence of the $M=5.4$ earthquake the seismicity of this region correlated with the lake level, implying the presence of fluids and delayed transfer of pore pressure. The delay is 120 days for deep seismicity and 60 days for the shallow activity.

Seismicity in the Aswan reservoir is controlled by the Kalabsha Fault (Fig. 2), particularly at the intersection between the North–South and East–West fault systems. According to Byerlee [32], groundwater plays a major role in fault friction, by triggering shallow earthquakes. Shallow earthquakes (<15 km) in the area are controlled by the fluids present along the fault plane. The mechanism involves pore water pressure inducing a reduction of the normal stress across the fault and allowing slip to occur, with the release of ambient stress. The fault creeps from the conductive (ductile) zone and propagates to the brittle material (i.e., granite) at the border of the resistive zone.

The horizontal extension of the hypocenters indicates that a system of vertical (or perhaps ***en échelon***) fault planes exists parallel to the others. This distribution is believed to be the cause for the laterally extensive conductive body observed.

7. Summary and conclusion

On the basis of the MT profile at nine stations, the main geoelectrical features of the area can be summarised as follows:

- The high resistivity region consists of two main zones. Between them (Fig. 4), a 3-km thick conductor of at least 5 km depth occurs in the tectonically weak zone (fractured fault/strike slip).
- The source of the deep, very highly conductive anomaly could be the presence between 6 and 16 km depth of heavily mineralized crustal fluids having penetrated for a long time along the fractured basement rocks and accumulated in the faults. Total dissolved solids in the pore fluid are likely to exceed those of sea water.
- Periodically these faults supply fluids to the surrounding dry rocks, allowing the sudden release of seismic energy.

Acknowledgments

This research project received financial support from the Swiss National Science Foundation (2100-65188). It was a great opportunity to carry out MT soundings in an area with a high-quality, dense seismic data catalogue extending over 20 years. We are grateful to Dr H. Awad for providing this earthquake catalogue.

References

[1] R.M. Kebeasy, M. Maamon, E.M. Ibrahim, Aswan Lake induced earthquake, Bull. Int. Inst. Seismol. Earthquake Eng., Tsukuba 19 (1982).
[2] D.W. Simpson, W.S. Leith, C.H. Scholz, Two types of reservoir-induced seismicity, Bull. Seismol. Soc. Am. 75 (1988) 2025–2040.
[3] D. Rooney, V. Hutton, A magnetotelluric and magnetovariational study of the Gregory Rift Valley, Kenya, Geophys. J. R. Astron. Soc. 51 (1977) 91–119.
[4] D. Bailey, K.A. Whaler, T. Zengeni, P.C. Jones, O. Gwavava, A magnetotelluric model of the Mana Pools basin, northern Zimbabwe, J. Geophys. Res. 105 (B5) (2000) 11185–11202.
[5] S. Hautot, P. Tarits, K. Whaler, B. Le Gall, J.J. Tiercelin, C. Le Turdu, Deep structure of the Baringo rift basin (Central Kenya) from three-dimensional magneto-telluric imaging: implications for the rift evolution, J. Geophys. Res. 105 (B10) (2000) 23,493–23,518.
[6] F. Simpson, A three-dimensional electromagnetic model of the southern Kenya Rift: departure from two dimensionality as a possible consequence of a rotating stress field, J. Geophys. Res. 105 (B8) (2000) 19,321–19,334.
[7] O. Ritter, U. Weckmann, T. Vietor, V. Haak, A magnetotelluric study of the Damara Belt in Namibia: 1. Regional scale conductivity anomalies, Phys. Earth Planet. Inter. 138 (2003) 71–90.
[8] U. Weckmann, O. Ritter, V. Haak, A magnetotelluric study of the Damara Belt in Namibia: 2. MT phases over 90° reveal the internal structure of the Waterberg Fault/Omaruru Lineament, Phys. Earth Planet. Inter. 138 (2003) 91–112.
[9] R.L. Mackie, D.W. Livelybrooks, T.R. Madden, J.C. Larsen, A magnetotelluric investigation of the San Andreas fault at Carrizo Plain California, Geophys. Res. Lett. 24 (1997) 1850–1874.
[10] M.J. Unsworth, P.E. Malin, G.D. Egbert, J.R. Booker, Internal structure of the San Andreas Fault at Parkfield, California, in: Geology, vol. 25, 1997, pp. 359–362.
[11] M.J. Unsworth, G.D. Egbert, J. Booker, High resolution electromagnetic imaging of the San Andreas Fault in central California, in: J. Geophys. Res., vol. 104, 1999, pp. 1131–1150.
[12] M.J. Unsworth, P. Bedrosian, M. Eisel, G.D. Egbert, W. Siripunvaraporn, Along strike variations in the electrical structure of the San Andreas Fault at Parkfield, California, Geophys. Res. Lett., vol. 29, 2000, pp. 3021–3024.
[13] P.A. Bedrosian, M.J. Unsworth, G.D. Egbert, Magnetotelluric imaging of the creeping segment of the San Andreas Fault near Hollister, Geophys. Res. Lett. 29 (11) (2002) 1506.

[14] S.K. Park, J.J. Roberts, Conductivity structure of the San Andreas Fault, Parkfield, revisited, Geophys. Res. Lett. 30 (16) (2003) 1842.
[15] C. Lemonnier, G. Marquis, F. Perrier, J.-P. Avouac, G. Chitrakar, B. Kafle, S. Sapkota, U. Gautam, D. Tiwari, M. Bano, Electrical structure of the Himalaya of central Nepal; high conductivity around the mid-crustal ramp along the MHT, Geophys. Res. Lett. 26 (21) (1999) 3261–3264.
[16] V.N. Pham, P. Bernard, D. Boyer, G. Chouliaras, J.-L. Le Mouël, G.N. Stravrakakis, Electrical conductivity and crustal structure beneath the central Hellenides around the Gulf of Corinth (Greece) and their relationship with the seismotectonics, Geophys. J. Int. 142 (2000) 948–969.
[17] H.K. Gupta, S.V.S. Sarma, T. Harinarayan, G. Virupakshi, Fluids below the hypocentral region of Latur earthquake, India: geophysical indicators, Geophys. Res. Lett. 23 (1996) 1569–1572.
[18] M. Mekkawi, J.R. Grasso, P.A. Schnegg, Seismicity patterns at Lake Aswan, Egypt, 1982–2001, Bull. Seis. Soc. Am. 94 (2) (2004) 479–492.
[19] X. Wu, I.J. Ferguso, A.G. Jones, Magnetotelluric response and geoelectric structure of the Great Slave Lake shear zone, Earth Planet. Sci. Lett. 196 (2001) 35–50.
[20] R. Said, The Geology of Egypt, Elsevier, Amsterdam, 1962, 377 pp.
[21] B. Issawi, Geology of Nubia west area, western desert, Annals of the Geological Survey of Egypt (1978).
[22] B. Issawi, Geology of the southwestern desert of Egypt, Ann. Geol. Surv. Egypt (1982).
[23] E.M. El-Shazly, The Geology of the Egyptian Region, 1977, 193–207 pp.
[24] P. Andrieux, G. Clerc, P. Tort, Capteur magnétometrique triaxial pour la prospection magnétotellurique artificielle entre 4 Hz et 4 kHz, Phys. Appl. 9 (1974) 183–190.
[25] J. Filloux, Instrumentation and experimental methods for oceanic studies, in: J. Jacobs (Ed.), Geomagnetism, vol. 1, Academic Press, London, 1987.
[26] P.-A. Schnegg, On-line selection of audio-magnetotelluric data with a digital signal processor, 10th Workshop on Electromagnetic Induction in the Earth, Ensenada, 1990.
[27] R.W. Groom, K. Bahr, Correction for near surface effects: decomposition of the magnetotelluric impedance tensor and scaling corrections for regional resistivities: a tutorial, Surv. Geophys. 13 (1992) 341–379.
[28] W. Siripunvaraporn, G. Egbert, An efficient data-subspace inversion method for 2-D magnetotelluric data, Geophysics 65 (2000) 791–803.
[29] R.M. Kebeasy, A.A. Gharib, Active fault and water loading are important factors in triggering earthquake activity around Aswan Lake, J. Geodyn. 14 (1991) 73.82.
[30] K. Evans, J. Beavan, D. Simpson, Estimating aquifer parameters from analysis of forced fluctuations in well level: an example from the Nubian formation near Aswan, Egypt: 1. Hydrogeological background and large-scale permeability estimates, J. Geophys. Res. 96 (B7) (1991) 12127–12137.
[31] R.S. Stein, The role of stress transfer in earthquakes occurrence, Nature 402 (1999) 605–609.
[32] J. Byerlee, Friction, over pressure and fault normal compression, Geophys. Res. Lett. 17 (1990) 2109–2112.